DMD Fast Forward. Published on November 28, 2006 as doi: 10.1124/dmd.106.011551
This article has not been copyedited and formatted. The final version may differ from this version.

METABOLISM OF MK-0524, A DP1 ANTAGONIST, IN MICROSOMES AND HEPATOCYTES FROM PRECLINICAL SPECIES AND HUMANS

Brian J. Dean, Bindhu Karanam, Steve Chang, Maria Victoria Silva Elipe, Yuan-Qing Xia, Matt Braun, Eric Soli, Yuming Zhao and Ronald B. Franklin

Department of Drug Metabolism
Merck Research Laboratories
Rahway, New Jersey 07065

Running title: In Vitro Metabolism of MK-0524

Corresponding author:

Bindhu Karanam

Merck Research Laboratories

Department of Drug Metabolism

RY80E-200

P.O. Box 2000

Rahway, NJ 07065, USA

Phone: 732-594-3117

FAX: 732-594-5390

Email: Bindhu_Karanam@merck.com

Number of text pages: 31

Number of tables: 5

Number of figures: 9

Number of references: 18

Number of words:

Abstract: 257

Introduction: 348

Discussion: 596

Abbreviations: DP1, prostaglandin D_2 receptor 1; MK-0524, [(3r)-4-(4-chlorobenzyl)-7-fluoro-5-(methylsulfonyl)-1,2,3,4-tetrahydrocyclopenta[b]indol-3-yl]acetic acid; UGT, UDP-glucuronosyltransferases.

Abstract

MK-0524 is a potent orally-active human DP1 (prostaglandin D_2 receptor 1) antagonist that is currently under development for the prevention of niacin-induced flushing. The major in vitro and in vivo metabolite of MK-0524 is the acyl glucuronic acid conjugate of the parent compound, **M2**. To compare metabolism of MK-0524 across preclinical species and human, studies were undertaken to determine the *in vitro* kinetic parameters (K_m and V_{max}) for the glucuronidation of MK-0524 in Sprague-Dawley rat, beagle dog, cynomolgus monkey and human liver microsomes, human intestinal microsomes and in recombinant human UGTs. A comparison of K_m values indicated that UGT1A9 has the potential to catalyze the glucuronidation of MK-0524 in the liver, whereas UGTs 1A3 and 2B7 have the potential to catalyze the glucuronidation in the intestine. MK-0524 also was subject to Phase I oxidative metabolism; however the rate was significantly lower than that of glucuronidation. The rate of phase I metabolism was ranked as follows: rat ~ monkey > human intestine > dog > human liver with qualitatively similar metabolite profiles across species. In all cases, the major metabolites were the monohydroxylated epimers (**M1** and **M4**), and the keto- metabolite, **M3.** Use of inhibitory monoclonal antibodies and recombinant human CYPs suggested that CYP3A4 was the major isozyme involved in the oxidative metabolism of MK-0524, with a minor contribution from CYP2C9. The major metabolite in hepatocyte preparations was the acyl glucuronide, **M2,** with minor amounts of **M1**, **M3**, **M4** and their corresponding glucuronides. Overall, the *in* vivo metabolism of MK-0524 is expected to proceed via glucuronidation, with minor contributions from oxidative pathways.

DMD Fast Forward. Published on November 28, 2006 as DOI: 10.1124/dmd.106.011551
This article has not been copyedited and formatted. The final version may differ from this version.

INTRODUCTION

Cardiovascular disease, associated with atherosclerosis, is the most common cause of death in the US. Major risk factors include elevated levels of low-density lipoprotein cholesterol (LDL-C), low levels of high-density lipoprotein cholesterol (HDL-C) and elevated triglyceride (TG) levels. Niacin (nicotinic acid) is a member of the vitamin B complex. It is commonly used as a dietary supplement in milligram quantities and as a plasma lipid-modifying drug in gram doses. Niacin increases HDL cholesterol while decreasing plasma concentrations of VLDL (very low-density) and LDL cholesterol (Shepherd et al, 1979, Knoop et al, 1999). Clinical trials have demonstrated the efficacy of niacin in the management of coronary heart disease when used alone or in combination with other lipid-altering drugs such as statins (Zhao et al, 2004, Rubenfire et al, 2004).

A major side effect of niacin is the development of cutaneous vasodilation, resulting in flushing of the upper body and face, immediately following dosing (Vogt et al, 2006). Since these effects are prevalent even at pharmacologically relevant doses, they have limited the widespread use of niacin. Studies have demonstrated that niacin-induced flushing could be reduced by cyclooxygenase inhibitors such as naproxen and indomethacin, suggesting the role of prostaglandins in vasodilation (Gentile et al, 1985, Eklund et al, 1979, Morrow et al, 1992). MK-0524, [(3R)-4-(4-chlorobenzyl)-7-fluoro-5-(methylsulfonyl)-1,2,3,4-tetrahydrocyclopenta[B]indol-3-yl]acetic acid, is a selective antagonist of DP1 (prostaglandin D2 receptor 1), with an IC_{50} value of 1.1 nM in a mouse DP1 functional assay (unpublished results). MK-0524 has also been shown to block niacin-induced vasodilation in the mouse by ~80% (Cheng et al, 2006). Clinical studies have demonstrated the efficacy of MK-0524 in reducing flushing symptoms when

administered prior to an oral dose of immediate-release niacin (500 mg) and is currently under development for this purpose (Cheng et al, 2006). The objective of this study was to delineate the comparative in vitro metabolism pathways of MK-0524 using microsomal preparations and hepatocytes isolated from rat, dog, monkey, and humans. Furthermore, studies were also conducted to identify the CYP and UGT isoforms responsible for the in vitro metabolism of MK-0524 in humans to aid in designing clinical studies.

DMD Fast Forward. Published on November 28, 2006 as DOI: 10.1124/dmd.106.011551
This article has not been copyedited and formatted. The final version may differ from this version.

MATERIALS AND METHODS

Materials

[Methylsulfonyl-^{14}C]MK-0524 and its acyl glucuronide (**M2**) were synthesized by the Labeled Compound Synthesis Group, Department of Drug Metabolism, Merck Research Laboratories, Rahway, NJ. A solution of [^{14}C]MK-0524 was prepared by a 1:10 dilution (v/v) from a stock to yield a solution with a specific activity of 0.12 mCi/mg (243 μg/mL or 29.2 μCi/mL). MK-0524 was synthesized by Process Research, Merck Research Laboratories, Rahway, NJ. **M1**, **M2**, **M3** and **M4** standards were obtained from Merck Frosst, Montreal, Canada (Nicoll-Griffith et al, in press). Recombinant human UDP-glucuronosyltransferases (UGTs 1A1, 1A3, 1A8, 1A9, 1A10 and 2B7) and CYPs 1A1, 2A6 and 2E1 were purchased from BD Gentest, Woburn, MA. Other recombinant human CYPs were obtained from the Department of Drug Metabolism, Merck Research Laboratories, West Point, PA. All CYPs contained NADPH-cytochrome P450 reductase. Sprague-Dawley rat, beagle dog and rhesus monkey liver microsomes were prepared in-house within the Department of Drug Metabolism, Rahway, NJ. Cynomolgus monkey (IVT batch #M00301-109) and human (IVT batch #X05841 Lot RDX, mixed gender, n=50) liver microsomes (used only for determination of kinetic parameters for glucuronidation), and beagle dog and human cryopreserved hepatocytes were purchased from In Vitro Technologies, Baltimore, MD. Human intestinal microsomes (HJM0040 0402991 SB, from a 42 year old male) were obtained from Tissue Transformation Technologies, Edison, NJ. UDPGA, saccharic acid-1,4-lactone, alamethicin, glucose 6-phosphate, $NADP^+$, glucose-6-phosphate dehydrogenase, testosterone and NADPH were purchased from Sigma Chemicals, St. Louis, MO. All solvents were of Optima grade

obtained from Fisher Scientific, Pittsburgh, PA. Sprague-Dawley rat and rhesus monkey hepatocytes were prepared in-house following standard isolation protocols.

Methods

Kinetics of Glucuronidation of MK-0524

All reactions were performed in polystyrene 96 well plates (Costar). MK-0524 (25 mM, dissolved in 75% aqueous acetonitrile) was serially diluted to make 12 working standard solutions. The reaction mixture (200 µl) consisted of the substrate, MK-0524 (0.3 to 625 µM), 50 mM 1,3-Bis[tris(hydroxymethyl)methylamino]propane buffer (pH 7.1), 10 mM $MgCl_2$, 10 mM saccharic acid-1,4-lactone, alamethicin (1 µg per 10 µg protein) and liver and intestinal microsomes or membrane preparations of recombinant UGTs (5 µg to 20 µg protein). The reaction mixtures were preincubated for 15 min at 37°C with mixing on a Boekel "Jitterbug" incubator, and the reactions were initiated by the addition of 2 mM UDPGA. Reactions were quenched at 0, 10, 30 or 90 min with 20 µl 50% acetic acid followed by 100 µl acetonitrile. Samples were spun in a centrifuge to remove particulate matter prior to HPLC analysis. For K_m and V_{max} determinations, substrate turnover was maintained to approximately 20% to ensure linear conditions for metabolism. Due to the poor aqueous solubility of the compound (0.06 mg/mL, internal Merck document), a visual check was performed on all samples (UV clear plates). Only data from samples analyzed by HPLC, determined to be in solution (final concentrations up to 40 µM) were used for kinetic determinations.

NADPH-dependent Phase I Metabolism

Phase I metabolism of [^{14}C]MK-0524 (5 μM) was studied in Sprague-Dawley rat, beagle dog, rhesus monkey, and human liver microsomes. Incubations consisted of microsomes (2 mg protein/mL) suspended in 100 mM potassium phosphate buffer (pH 7.4) and 10 mM $MgCl_2$. The reactions were initiated by the addition of an NADPH-regenerating system consisting of 1 mM $NADP^+$, 10 mM glucose-6-phosphate and 0.7 units/ml glucose-6-phosphate dehydrogenase. Reactions were carried out for 30 or 60 min at 37°C and stopped at appropriate time points by adding half the volume of acetonitrile containing 2% aqueous formic acid. Following vortex-mixing and spinning in a centrifuge (14,000 rpm for 10 min), supernatants were analyzed by LC-MS/MS with on-line radiometric detection (β-RAM, IN/US). Kinetic experiments with MK-0524 were performed under linear microsomal protein and incubation time conditions in a 96-well format as described above.

Combined Phase I and II Metabolism

To study the in vitro metabolism of MK-0524 under combined Phase 1 and 2 conditions, (rhesus monkey liver microsomes only), 2 mg protein/mL of microsomal protein was suspended in 100 mM potassium phosphate buffer (pH 7.4) and 10 mM $MgCl_2$, were preincubated in the presence of 0.1 mg/mL alamethicin for 15 min. Following the pre-incubation period, [^{14}C]MK-0524 (5 μM) was added to the microsomal mixture, along with 5 mM saccharic acid-1,4-lactone, an inhibitor of β-glucuronidase, and incubated for a further 5 min at 37°C. The reactions were initiated by the addition of 5 mM UDPGA and an NADPH-regenerating system consisting of 1 mM NADP, 10 mM glucose-6-phosphate and 0.7 units/ml glucose-6-phosphate dehydrogenase. The sample mixture was incubated for 15 or 30 min at 37°C. Reactions were stopped by adding half the volume

of acetonitrile containing 2% aqueous formic acid in order to stabilize the acyl glucuronide(s). Samples were vortex-mixed and spun in a centrifuge (14,000 rpm for 10 min at room temperature). The supernatants were analyzed by LC-MS/MS and an on-line radiometric detector (β-Ram). For NMR analysis of **M6**, scaled-up incubations of [^{14}C]MK-0524 with monkey liver microsomes in the presence of NADPH and UDPGA were set up as above. Samples were analyzed by HPLC on a SB-Phenyl column as described under Bioanalytical Methods. Radioactive peaks corresponding to the peak for **M6** were collected based on radioactivity, evaporated to dryness under nitrogen and reconstituted in acetonitrile/water (50;50, v/v). Following HPLC reanalysis on a pristine column under similar conditions as above, the pooled fractions were concentrated under nitrogen and subjected to LC-MS/MS and NMR analysis.

CYP Isoform Determination

All reactions were performed in 96-well plate format with duplicate time points. The final 200 µl reaction contained: substrate (10 µM), 100 mM potassium phosphate (pH 7.4), 10 mM $MgCl_2$, and recombinant CYP microsomes (20 pmol P450 protein). Reaction mixtures were preincubated for 15 min at 37°C, with mixing on a Boekel "Jitterbug" incubator and reactions initiated by the addition of 1 mM NADPH. Reactions were quenched after 0, 15, 30 or 90 min with 20 µl 50% aqueous acetic acid followed by 100 µl acetonitrile. Samples were spun in a centrifuge (14,000 rpm for 10 min at room temperature) prior to HPLC analysis. To determine the effect of anti-CYP monoclonal antibodies on the reaction, incubations were conducted in the presence of 2.5, 5, 10 or 20 µl of inhibitory CYP3A4 or CYP2C8/9 antibodies or 40 µl of a CYP3A4 and CYP2C8/9 mixture.

DMD Fast Forward. Published on November 28, 2006 as DOI: 10.1124/dmd.106.011551
This article has not been copyedited and formatted. The final version may differ from this version.

Metabolism in Hepatocytes

[^{14}C]MK-0524 (10 μM) was incubated with a suspension of freshly isolated Sprague-Dawley rat and rhesus monkey hepatocytes and cryopreserved beagle dog and human hepatocytes (1 x 10^6 cells/mL) in a hepatocyte incubation media (IVT, Baltimore, MD) for 0, 60, 120 or 240 min at 37°C under an atmosphere of 95% O_2/ 5% CO_2. Reactions were stopped by adding half the volume of acetonitrile containing 2% aqueous formic acid. Samples were frozen (-70°C for one hour) and allowed to thaw at room temperature. After vortex-mixing and spinning in a centrifuge (14,000 rpm for 10 min at room temperature), the supernatants were analyzed by LC-MS/MS with on-line radiometric detection (β–Ram). In order to isolate **M2** and **M8** for NMR analyses, scaled up incubations were conducted with the parent compound and monkey hepatocyte suspensions as described above. Sample analysis was as described for the isolation of **M3** from monkey microsomal incubations.

NMR Analysis

NMR analysis was carried out on **M3** (a synthetic standard) and **M6** (~24 μg based on radioactivity) isolated from an incubation of [^{14}C]MK-0524 with monkey liver microsomes in the presence of NADPH and UDPGA. The spectra were recorded in deuterated acetonitrile (CD_3CN) : deuterated water (D_2O) 2:3, v/v, in 0.15 ml at 25°C (298 K) in 3 mm NMR tubes (Nalorac 3 mm indirect detection gradient probe) and run at 600 and 150 MHz for ^{1}H and ^{13}C, respectively, using a Varian Unity Inova 600 spectrometer (Palo Alto, CA). Chemical shifts were reported in the δ scale (ppm) by assigning the residual CD_2HCN solvent peak to 1.93 and 1.39 ppm for ^{1}H and ^{13}C, respectively. The 2D ^{1}H-^{1}H COSY and ROESY spectra were acquired with a spectral width of 5397.4 Hz into 1K data points in f2, with 270 increments in the f1 dimension.

DMD Fast Forward. Published on November 28, 2006 as DOI: 10.1124/dmd.106.011551
This article has not been copyedited and formatted. The final version may differ from this version.

Solvent suppression was carried out by pre-saturation. The mixing time for 2D ^{1}H-^{1}H ROESY was 0.3 sec. The delays between successive pulses were 0.6 and 1.0 sec for 2D ^{1}H-^{1}H COSY and ROESY, respectively.

In a separate set of experiments, NMR analysis was carried out on the synthetic standard of MK-0524 (1 mg) and its two major metabolites **M2** and **M8** (~50 μg based on radioactivity) isolated from the incubation of [^{14}C]MK-0524 in monkey hepatocytes. The ^{1}H and ^{13}C spectra were recorded as above. The 2D ^{1}H-^{1}H COSY and ROESY spectra were acquired with a spectral width of 4197.9 Hz into 1K data points in f2, with 419 increments in the f1 dimension. Solvent suppression was carried out by pre-saturation. The mixing time for 2D ^{1}H-^{1}H ROESY was 0.3 sec. The delays between successive pulses were 0.5 and 1.0 sec for 2D ^{1}H-^{1}H COSY and ROESY, respectively. The 2D ^{1}H-^{13}C HSQC experimental data were acquired with spectral widths of 4197.9 and 30154.5 Hz for ^{1}H and ^{13}C dimensions, respectively, 1K data points in f2, and with 301 increments in f1 dimension. The 90° pulses were 5.35 and 12.0 μs for ^{1}H and ^{13}C, respectively. The delay during acquisition was 3.6 msec ($1/2J_{CH}$).

Bioanalytical Methods

For the glucuronidation reactions, extracts of reaction mixtures were analyzed on a 3 x 50 mm Luna 3 μm Phenyl-Hexyl column (Phenomenex, Torrance, CA) with UV detection (Shimadzu LC10A system) at 311 nm. Mobile phase A consisted of 10 mM aqueous ammonium acetate containing 0.1 % acetic acid and mobile phase B consisted of acetonitrile: methanol, 92.8/7.2, v/v, containing 7.2 mM ammonium acetate and 0.1% acetic acid. The separation of the acyl glucuronide, **M2**, from the parent compound was performed over 7.5 min using linear gradient elution from 35% to 95% B at a flow rate of 1 mL/min.

Turnover was calculated as the glucuronide peak area divided by the sum of glucuronide and parent peak areas. Both K_m and V_{max} parameters were calculated using Enzyme Kinetics!Pro software (ChemSW, Inc., Fairfield, CA) with the least squares method and by fitting the data to the Michaelis-Menten equation. Metabolic profiles of [^{14}C]MK-0524 from microsomal and hepatocyte incubations were obtained using a 4.6 x 250 mm Zorbax 5 μm SB-Phenyl column (Agilent Technologies) with UV detection at 311 nm and monitoring the radioactive eluate using a β-Ram detector. Mobile phases were as above. The column was eluted over a 40-min period with a linear gradient from 25% to 65% B. All HPLC separations were carried out at room temperature at a flow rate of 1 ml/min.

Metabolite identification was established by comparison to synthetic standards, where available, using retention time comparison as well as mass spectral data. LC-MS analysis was performed on a Perkin Elmer Sciex API 2000 with Turbo-IonSpray in the negative ionization mode.

For metabolite identification from hepatocyte and microsomal incubations, LC-MS experiments were conducted using a Finnigan Deca XP ion trap mass spectrometer that was interfaced with a Perkin-Elmer autosampler (Series 200) and a Shimazdu HPLC system consisting of LC-10AD *VP* pumps, and a SCL-10A *VP* system controller. Both LC-MS and LC-MS^n experiments were carried out using the electrospray interface operating in the negative ion mode. The source temperature was maintained at 300°C and the spray voltage was 4,500 V. For MS^2 experiments, relative collision energy of 35 eV was used. Data-dependent scans were used to assist in the detection of metabolites. A 4.6 x 250 mm 5μm Zorbax RX-C18 column (Agilent Technologies, Wilmington, DE) was used for HPLC separation. The flow rate was 1 mL/min and the LC effluent was

split, with one-fourth directed into the mass spectrometer, and the remainder into the radiometric detector (β-Ram). Mobile phase and gradient conditions were as used above. Identification of the acyl glucuronide metabolite, **M2**, the mono-hydroxylated metabolites **M1** and **M4**, and the keto-metabolite **M3**, were confirmed using authentic standards.

RESULTS

Glucuronidation of MK-0524

The *in vitro* glucuronidation of MK-0524 was examined in liver microsomes from male Sprague-Dawley rat, beagle dog, cynomolgus monkey and human (microsomes from mixed genders). Also, glucuronidation in human intestinal microsomes was studied. The V_{max}, K_m and intrinsic clearance (V_{max}/K_m) values are listed in Table 1. A species comparison of the *in vitro* intrinsic clearance values for the glucuronidation of MK-0524 in liver microsomes followed the rank order: rat > monkey ~ dog > human and were 262, 100, 80 and 22 μL/min/mg, respectively. The intrinsic clearance in human intestinal microsomes was similar to that in human liver (~27 μl/min/mg).

The rates of glucuronidation of MK-0524 by different human UGT isoforms are depicted in Table 2. The data indicates that UGT1A3, UGT2B7 and UGT1A9 exhibited the highest rate of glucuronidation as a function of the amount of protein used in the incubations - 413, 106 and 87 pmol/min/mg, respectively. The rate of metabolism with UGT1A1 was lower than the other isoforms, 8 pmol/min/mg protein, whereas UGT1A8 and UGT1A10 did not exhibit any turnover of the compound. In order to determine the major UGT isoform(s) involved in the glucuronidation of MK-0524 in humans, the apparent K_m values in recombinant human UGT isoforms were determined and compared to those values obtained in human liver and intestinal microsomes. The K_m for UGT1A9 (13 μM) was similar to the K_m in human liver microsomes (19 μM) indicating that UGT1A9 was the isoform that most likely had the potential to catalyze the glucuronidation of MK-0524 in the liver. Also, 1-hydroxypyrene, an avid substrate for UGT1A9 (Luukkanen et al, 2001), was shown to inhibit the glucuronidation of MK-0524

DMD Fast Forward. Published on November 28, 2006 as DOI: 10.1124/dmd.106.011551
This article has not been copyedited and formatted. The final version may differ from this version.

in human liver microsomes by 92% at a concentration of 125 μM. The calculated IC_{50} value was 27 μM (data not shown).

In the case of human intestine, the K_m for MK-0524 glucuronidation in human intestinal microsomal preparation, 7 μM, was similar to that estimated for UGT1A3 (K_m = 6.6 μM) and UGT2B7 (K_m = 3.3 μM), suggesting that both these isoforms may play a role in the glucuronidation of MK-0524 in the gut.

NADPH-Dependent Metabolism of MK-0524

The NADPH-dependent metabolism of [^{14}C]MK-0524 was investigated with liver microsomes from rat, beagle dog, rhesus monkey and human (metabolic pathway depicted in Fig 1). The poor solubility of the parent compound in microsomal incubation precluded the estimation of definitive in vitro kinetic parameters. Nevertheless, the rate of Phase 1 metabolism of MK-0524 with human liver microsomes was considerably slower than glucuronidation, as depicted in Figure 2. Metabolites formed and radioactive metabolite profiles from liver microsomal incubations of MK-0524 (10 μM) were qualitatively similar across species and are shown in Table 3 and Figure 3. Identification of major metabolites was based on comparison with standards, where available, and LC-MS/MS analysis (see below). The major oxidative metabolites in all species were the monohydroxylated epimers, **M1** and **M4**. Trace amounts of the keto- metabolite, **M3**, were formed in rat, monkey and human microsomes. Rat liver microsomes also generated minor amounts of an *N*-dealkylated metabolite of a monohydroxylated product, **M5**. An additional oxidized metabolite, **M7**, was present as a minor metabolite in all species; however, the exact structure has not yet been identified. The major metabolites formed in human intestinal microsomes also were **M1** and **M4** (Fig 4). The metabolism of MK-0524 was also studied in the presence of both NADPH and UDPGA in monkey liver

DMD Fast Forward. Published on November 28, 2006 as DOI: 10.1124/dmd.106.011551
This article has not been copyedited and formatted. The final version may differ from this version.

microsomes (Fig 5). The major metabolite was the acyl glucuronide, **M2**, along with glucuronides of **M1,** designated as **M9** and **M10**. Also identified by mass spectrometry were minor amounts of the glucuronides of **M4** designated as **M11** or **M12** and a glucuronide of **M3**, **M6**, the structure of which was identified by NMR analysis (see below).

Incubations of MK-0524 with recombinant human CYPs suggested the major involvement of CYP3A4, with a minor contribution from CYP2C9, in the formation of the two major Phase I metabolites, **M1** and **M4** (Table 4 and Fig 6). The rates of formation of **M1** by CYP3A4 and CYP2C9 were 19.2 and 1.9 pmol/pmol*hr, respectively. The rates of formation of **M4** by CYP3A4 and CYP2C9 were 27 and 2.4 pmol/pmol*hr, respectively. There was negligible metabolism of MK-0524 by recombinant CYP1A1, 2A6, 2C19, 2D6 and 2E1 microsomes. The involvement of CYP3A4 and CYP2C9 was confirmed by conducting human liver microsomal incubations in the presence of monoclonal antibodies to these two CYPs. At the highest concentration of antibody used (100 μL/mg microsomal protein), approximately 85% and 15% of MK-0524 metabolism in human liver microsomes was inhibited by anti-CYP3A4 and anti-2C8/9 antibodies, respectively (Fig 7). Incubation with a mixture of anti-CYP3A4 and anti-2C8/9 antibodies resulted in 98% inhibition of Phase 1 metabolism of MK-0524.

Hepatocyte Incubations

Following incubations of MK-0524 (10 μM) with Sprague-Dawley rat, beagle dog, rhesus monkey and human cryopreserved hepatocyte suspensions, substantial turnover of the parent compound was observed, with qualitatively similar metabolite profiles across the species. Identification of major metabolites was based on comparison with standards,

DMD Fast Forward. Published on November 28, 2006 as DOI: 10.1124/dmd.106.011551
This article has not been copyedited and formatted. The final version may differ from this version.

where available, and LC-MS/MS analysis (see below). Representative metabolite profiles following 4-hr incubation are shown in Figure 8. The major metabolites in all species were **M2**, the acyl glucuronide of MK-0524, and its rearranged products. The latter metabolites were identified by NMR analysis (see below) to be a mixture of the stable α-anomer, **M8**, and at least one additional migration product. In addition, Phase I metabolites, such as **M1, M4** and **M3**, also were identified as minor metabolites in rat, monkey and human hepatocytes. Also, glucuronic acid conjugates of **M1**, **M4** and **M3** were detected in small amounts in these species and were designated as **M9** or **M10**, **M11** or **M12**, and **M6**, respectively (Table 3). Also present in small amounts in rat hepatocytes, was **M7**. **M6**, the glucuronide conjugate of **M3,** was present in rat, monkey and human hepatocytes.

LC-MS/MS Analysis

The parent compound, MK-0524, gave a deprotonated molecular ion [M-H$^-$] at an *m/z* 434 (Fig 9, Table 5). The collision-induced dissociation (CID) spectrum yielded fragment ions with *m/z* at 416 and 390 which corresponded to loss of water (18 Da), and carbon dioxide (44 Da) from the parent. Additionally, a fragment ion at *m/z* 278 corresponded to the loss of the chlorophenyl moiety from m/z 390.

The acyl glucuronide metabolite of the parent compound and its rearranged isomer, **M2** and **M8**, respectively, gave deprotonated molecular ions [M-H$^-$] at *m/z* of 610, corresponding to an addition of 176 Da to the parent compound (*m/z* 434). Additional fragments were 434 (due to loss of m/z 176) and similar to those obtained from the parent compound (above), viz., m/z 278, 390 and 416 Da.

The hydroxylated epimers, **M1** and **M4**, gave rise to deprotonated molecular ion [M-H$^-$] at *m/z* of 450, indicative of the addition of 16 Da to the parent compound. Similar

fragments as above, which corresponded to losses of water and carbon dioxide, were observed at *m/z* 432 and 406, respectively. Furthermore, a major fragment ion at *m/z* 388 indicative of loss of water (18 Da) from *m/z* 406 was indicative of hydroxylation of the cyclopentane ring.

The keto derivative (**M3**) gave rise to a deprotonated molecular ion [M-H$^-$] at *m/z* 448, an addition of 14 Da on the parent compound, indicating an oxidation at an aliphatic position followed by further oxidation to a carbonyl. The major product ions were *m/z* 430 (loss of water) and *m/z* 404 (loss of carbon dioxide). Also, a major fragment at m/z 376 corresponded to the loss of 28 Da (CO) from *m/z* 404, was indicative of a keto group on the cyclopentane ring.

A minor metabolite, **M5**, was identified as the N-dealkylated derivative of a hydroxylated metabolite. It gave rise to a deprotonated molecular ion [M-H$^-$] at *m/z* 326, corresponding to a loss of 126 Da and addition of 16 Da to the mass of the parent compound. The CID spectrum of this metabolite yielded fragments at *m/z* 308 and 282 (loss of water (18 Da) and carbon dioxide (44 Da), respectively). Further loss of water from *m/z* 282 to yielded a major fragment at *m/z* 264, was indicative of an aliphatic hydroxyl group on the cyclopentane ring.

An oxidative metabolite, identified as **M7,** gave rise to a deprotonated molecular ion at m/z 432, corresponding to a loss of 2 Da from the parent molecule. The characteristic loss of carbon dioxide (44 Da) generated a major fragment at m/z 388. Also present was another fragment at m/z 262 formed as a result of the loss of the chloro-benzyl moiety (loss of 126 Da).

The acyl glucuronide conjugates of the hydroxylated metabolites (**M9**/**M10** and **M11**/**M12**) were observed at m/z **626**, corresponding to an addition of 176 Da to the mass

of the hydroxylated metabolites M1 and M4 (m/z 450). Further fragments obtained were similar to those obtained with M1 and M4, viz., at *m/z* 432, 406 and 388.

NMR Identification

The structure of **M2** (isolated from monkey liver microsomes fortified with UDPGA) was identified to be the acyl glucuronide of MK-0524, based on direct comparison of the proton (^{1}H) NMR of the synthetic standard. **M6** was isolated from the incubation of [^{14}C]MK-0524 with monkey liver microsomes in the presence of NADPH and UDPGA. The ^{1}H NMR analysis suggest it to be the 1-β-O-acyl glucuronide of **M3,** based on the following observations: protons at position 1 are absent, suggesting oxidation to the ketone, the chemical shift (5.36 ppm) and coupling constant (8.1 Hz) of the anomeric proton indicates a 1-β-O-acyl glucuronide and LC-MS data are consistent with the de-protonated molecular ion (*m/z* 624, [M+176-H]) (data not shown).

Incubation of [^{14}C]MK-0524 (50 μM) with monkey hepatocytes gave rise to two major chromatographic peaks (Figure 8); both of these were identified as glucuronide conjugates of the parent compound by LC-MS (*m/z* 610, $[M+176-H]^{-}$, for both peaks). One of the peaks was identified as **M2** by direct NMR comparison to the standard. The ^{1}H NMR of the second peak, designated as **M8**, indicated a mixture of two major components. COSY, ROESY and HSQC experiments were carried out to establish whether the components of that peak represented the acyl migration products derived from **M2** (data not shown). One of the components of **M8** was identified as an α-anomer based on the small coupling constant of the anomeric proton (5.18 ppm, 1H, J=3.7 Hz). Because of extensive signal overlap, however, the anomeric stereochemistry of the second component was not determined (4.52 to 4.58 ppm) (data not shown).

DISCUSSION

MK-0524, a novel DP1 antagonist that is under development for the treatment of niacin-induced flushing, was found to undergo extensive glucuronidation in hepatocytes and liver microsomes from preclinical species and humans. The rate of formation of the acyl glucuronide in microsomes was highest in the rat, followed by the monkey and dog, and then human intestine and liver. MK-0524 would be expected to undergo first pass metabolism in the gut, based on the propensity of the compound to undergo glucuronidation in vitro in human intestinal microsome preparations. Results from this paper complement the results of the studies conducted to evaluate the in vivo metabolism of MK-0524 in preclinical species wherein it was observed that the major route of elimination of the compound is via glucuronidation (Chang et al., manuscript submitted). Based on a comparison of the K_m values generated in vitro using recombinant UGTs, UGT1A9 has the potential to catalyze the glucuronidation of MK-0524 in the human liver and UGTs 1A3 and 2B7 have the potential to catalyze the glucuronidation in the human intestine. These three isoforms also exhibited higher rates of glucuronidation than those observed with UGT1A1, UGT1A8 and UGT1A10. However, comparison of the V_{max} values across these isoforms is not possible as accurate measurements of the UGT protein expression levels cannot be determined.

Glucuronidation is a principal step in the metabolic pathway for a wide variety of endogenous substrates and xenobiotics. Substrate specificities for UGTs are, however, broad and overlapping with several UGTs responsible for catalyzing specific reactions. However, some substrates have been shown to be selectively catalyzed by specific isoforms. Some examples of some of these are bilirubin, which is glucuronidated

selectively by UGT1A1 (Bosna et al., 1994), propofol by UGT1A9 (Burchell et al, 1995) and morphine 6-glcuronidation by UGT2B7 (Coffman et al, 1997; Stone et al, 1995). In the case of compounds such as MK-0524 wherein several recombinant UGT isoforms are involved, a comparison of kinetic parameters determined using expressed protein to those determined in human liver microsomal preparations is probably the best method to evaluate substrate specificity (Remmel et al, 1993). These determinations would probably be much more refined when specific monoclonal antibodies to specific human UGT isoforms become available. Many carboxylic acid-containing drugs, such as the nonsteroidal anti-inflammatory drugs, clofibric acid and valproic acid are glucuronidated by UGT2B7, which is a major isoform present in the liver and gut tissue (Jin et al, 1993, King et al, 2001). The data obtained with MK-0524 glucuronidation is consistent with the involvement of UGT2B7 being the primary UGT isoform in the gut, based on the similarity of the Km values for its glucuronidation in human gut preparation vs. recombinant UGT2B7, 7 vs. 3 μM, respectively.

MK-0524 was also susceptible to Phase I metabolism in liver microsomes from preclinical species and humans, however the extent was much lower than glucuronidation. The metabolism of MK-0524 was qualitatively similar in liver microsomes in preclinical species and humans. The major metabolites generated in all species were the mono-hydroxylated epimers, **M1** and **M4**. Smaller amounts of the keto-metabolite, **M3**, were also formed in all species. Using recombinant CYPs and monoclonal antibodies, it was concluded that the human CYPs involved in the Phase 1 metabolism of MK-0524 were CYP3A4 and CYP2C9.

The major metabolites of MK-0524 in hepatocyte preparations from the rat, dog, monkey and human were **M2** (the acyl glucuronide of MK-0524), its α-anomer, (**M8),** and other

products of acyl migration. The Phase I metabolites, **M1**, **M3**, **M4** and their respective acyl glucuronides were observed in trace amounts.

Overall, the *in vitro* metabolism of MK-0524 proceeded largely via glucuronidation.

ACKNOWLEDGEMENTS

The authors wish to thank Dr. Deborah Nicoll-Griffith, Yves Aubin, Claudio Sturino and other members of the Medicinal Chemistry Department of Merck Frosst for supplying the standards for **M1**, **M3** and **M4**.

REFERENCES

Bosma PJ, Seppen J, Goldhoorn B, Bakker C, Oude Elferink RP, Chowdhury JR, Chowdhury NR, and Jansen PL (1994) Bilirubin UDP-glucuronosyltransferase 1 is the only relevant bilirubin glucuronidating isoform in man. *J Biol Chem* **269:** 17960-17964.

Burchell B, Brierley CH, and Rance D (1995) Specificity of human UDP-glucuronosyltransferases and xenobiotic glucuronidation. *Life Sci* **57:** 1819-1831

Chang S, Karanam B, Reddy, V, Pereira T, Dean B and Franklin, R (submitted). The pharmacokinetics and disposition of MK-0524 a DP1 antagonist, in rats, dogs and monkeys.

Cheng K, Wu T-J, Wu KK, Sturino C, Metters K, Gottesdiener K, Wright SD, Wang Z, O'Neill G, Lai E and Waters MG (2006) Antagonism of the Prostaglandin D2 Receptor 1 Suppresses Nicotinic Acid-Induced Vasodilation in Mice and Humans. *Proc Natl Acad Sc.* 103(17):6682-6687.

Coffman BL, Rios GR, King CD, and Tephly TR (1997) Human UGT2B7 catalyzes morphine glucuronidation**.** *Drug Metab Dispos* **25:** 1-4.

Eklund, B., Kaijser, L., Nowak, J., and Wennmalm,A (1979) Prostaglandins contribute to the vasodilation induced by nicotinic acid. *Prostaglandins.* **17**:821–830.

Gentile.S, Rubba P, Persico M, Bronzino P, Marmo R and Faccenda F (1985) Improvement of the nicotinic acid test in the diagnosis of Gilbert's syndrome by pretreatment with indomethacin. *Hepatogastroenterology.* **32(6):**267-9.

Jin C, Miners JO, Lillywhite KJ, and Mackenzie PI (1993) Complementary deoxyribonucleic acid cloning and expression of a human liver uridine diphosphate-

glucuronosyltransferase glucuronidating carboxylic acid-containing drugs. *J Pharmacol Exp Ther* **264:** 475-479.

King C, Tang W, Ngui J, Tephly T, and Braun M (2001) Characterization of rat and human UDP-glucuronosyltransferases responsible for the in vitro glucuronidation of diclofenac. *Toxicol Sci* **61:** 49-53.

Knoop RH (1999) Drug treatment of lipid disorders. *N. Eng. J. Med*. **341**: 498-511.

Luukkanen, L., Mikkola J, Forsman T, Taavitsainen P and Elovaara E. (2001) Glucuronidation of 1-hydroxypyrene by human liver microsomes and human UDP-glucuronosyltransferases UGT1A6, UGT1A7, and UGT1A9: development of a high-sensitivity glucuronidation assay for human tissue. *Drug Metab Dispos*. **29**(8): 1096-101.

Morrow JD, Awad JA, Oates JA, Roberts LJ 2nd (1992) Identification of skin as a major site of prostaglandin D2 release following oral administration of niacin in humans. *J. Invest Dermatol*. **98 (5)**:812-5.

Nicoll-Griffith DA, Seto C, Aubin Y, Lévesque J-F, Chauret N, Day S, Silva JM, Trimble LA, Truchon JF, Bertelette C, Lachance N, Wang Z, Sturino C, Braun M, Zamboni R and Young RN. In vitro biotransformations of the prostaglandin D2 (DP) antagonist MK-0524 and synthesis of metabolites. In press.

Remmel RP and Burchell B (1993) Validation and use of cloned, expressed human drug metabolizing enzymes in heterologous cells for analysis of drug metabolism and drug-drug interactions. *Biochem. Pharmacol*. **46**:559-566 (1993).

Rubenfire M (2004) Safety and Compliance with Once-Daily Niacin Extended-Release/Lovastatin as Initial Therapy in the Impact of Medical Subspeciality on Patient

Compliance to Treatment (IMPACT) Study. *The American Journal of Cardiology*. **94**:306-311.

Shepherd J, Packard DJ, Patsch JR, Gotto AM, Jr, and Taunton OD (1979) Effects of nicotinic acid therapy on plasma high density lipoprotein subfraction distribution and composition and on apolipoptotein A metabolism. *J. Clin. Invest*. **63**:858-867.

Vogt A, Kassner U, Hostalek U, Steinhagen-Thiessen E (2006) On Behalf of the Nautilus Study Group, 2006. Evaluation of Safety and Tolerability of prolonged-release Nicotonic Acid in a Usual Care Setting. *Curr Med Res Opinion*. **22(2)**: 417-25.

Zhao X-Q, Morse JS, Dowdy AA, Heise N, DeAngelis D, Frohlich J, Chait A, Albers JJ, and Brown BG. (2004). Safety and Tolerability of Simvastatin plus Niacin in Patients with Coronary Artery Disease and Low High-Density Lipoprotein Cholesterol (The HDL Atherosclerosis Treatment Study). *The American Journal of Cardiology*. **93**:307-312.

Figure Legends

Figure 1. Proposed Metabolic Pathways for MK-0524

Figure 2. Comparison of UDPGA- and NADPH-Dependent Metabolism of MK-0524 by Human Liver Microsomes

Figure 3. Radiochromatograms Illustrating the Representative Metabolite Profiles of [^{14}C]MK-0524 in Incubations With NADPH-Enriched Male Rat, Dog, Rhesus Monkey, and Human Liver Microsomes

Figure 4. Radiochromatograms Illustrating Metabolite Profile of [^{14}C]MK-0524 Incubations With NADPH-Enriched Male Human Intestinal Microsomes

Figure 5. Metabolism of [^{14}C] MK-0524 in NADPH-Enriched Rhesus Monkey Liver Microsomes in the Absence (A) or Presence (B) of UDPGA

Figure 6. Radiochromatograms Illustrating the Metabolite Profiles of [^{14}C]MK-0524 Incubations With Recombinant Human CYP3A4 and CYP2C9 in the Presence of NADPH

Figure 7. Effect of Anti-CYP Monoclonal Antibodies on the NADPH-Dependent Metabolism of [^{14}C]MK-0524 by Human Liver Microsomes

Figure 8. Radiochromatograms Illustrating the Metabolism of [^{14}C] MK-0524 in Incubations with Rat, Dog, Rhesus Monkey and Human Hepatocytes

Figure 9. MS/MS spectrum of MK-0524 and assignments of its fragment ions.

DMD Fast Forward. Published on November 28, 2006 as DOI: 10.1124/dmd.106.011551
This article has not been copyedited and formatted. The final version may differ from this version.

TABLE 1

Mean Kinetic Parameters for the Glucuronidation of MK-0524 in Microsomal Preparations from Rat, Dog, Cynomolgus Monkey, Human Liver, and Human Intestine [a]

Species	V_{max} (pmol/min/mg)	K_m (μM)	V_{max}/K_m (μl/min/mg)
Rat Liver	1872	7	262
Dog Liver	1577	20	80
Cynomolgus Monkey Liver	1234	12	100
Human Liver	425	19	22
Human Intestine	184	7	27

[a] MK-0524 (0.3 to 40 μM) was incubated with liver microsomes in the presence of 2 mM UDPGA at 37°C. Values represent mean; n = 2

DMD Fast Forward. Published on November 28, 2006 as DOI: 10.1124/dmd.106.011551
This article has not been copyedited and formatted. The final version may differ from this version.

TABLE 2

Mean Apparent Kinetic Parameters for the Glucuronidation of MK-0524 with Recombinant Human UGTs [a]

Human UGT Isoform	App V_{max} (pmol/min/mg)	App K_m (μM)	App V_{max}/K_m (μl/min/mg)
1A1	8	1.9	4
1A3	413	6.6	62
1A8	nd	nd [b]	nd [b]
1A9	87	13.3	7
1A10	nd [b]	nd [b]	nd [b]
2B7	106	3.3	32

[a] MK-0524 (0.3 to 40 μM) was incubated with membrane preparations of recombinant human UGTs from baculovirus-infected cells (0.1 mg/mL) in the presence of 2 mM UDPGA at 37°C. Values represent mean; n = 2

[b] nd = not determined. No metabolite formation was observed.

DMD Fast Forward. Published on November 28, 2006 as DOI: 10.1124/dmd.106.011551
This article has not been copyedited and formatted. The final version may differ from this version.

TABLE 3

Metabolites of MK-0524 Detected in Liver Microsomes and Hepatocytes[a]

Metabolite[b]	RT[c]	$[M-H]^-$ [c]	MW[c]	RLM[c]	RH[c]	DLM[c]	DH[c]	MLM[c]	MH[c]	HLM[c]	HH[c]
MK-0524	32.9	434	435	√[d]	√	√	√	√	√	√	√
M1	20.6	450	451	√	√	√	ND	√	√	√	√
M2	17.6	610	611	ND	√	ND	√	ND	√	ND	√
M3	23.1	448	449	√	√	ND	ND	√	√	√	√
M4	21.9	450	451	√	√	√	ND	√	√	√	√
M5	10.4	326	327	√	ND	ND[e]	ND	√	ND	ND	ND
M6	12.1	624	625	ND	√	ND	ND	ND	√	ND	√
M7	31.3	432	433	√	√	√	ND	√	ND	√	ND
M8	18.4	610	611	ND	√	ND	√	ND	√	ND	√
M9	10.7	626	627	ND	√	ND	ND	ND	√	ND	√
M10	11.4	626	627	ND	√	ND	ND	ND	√	ND	√
M11	12.9	626	627	ND	√	ND	ND	ND	√	ND	√
M12	13.3	626	627	ND	√	ND	ND	ND	√	ND	√

[a] [^{14}C]MK-0524 was incubated with liver microsomes (and an NADPH-regenerating system) and with hepatocytes. Acetonitrile supernatants of the incubations were analyzed by LC-MS and LC-MS/MS (see text for details).

[b] See Fig.1 for chemical structures.

[c] RT = Retention time (min), $[M-H]^-$ = *m/z*, MW = Molecular weight (amu), RLM = rat liver microsomes, RH = rat hepatocytes, DLM = dog liver microsomes, DH = dog hepatocytes, MLM = rhesus monkey liver microsomes, MH = rhesus monkey hepatocytes, HLM = human liver microsomes, HH = human hepatocytes,

[d] √ = Denotes detected.

[e] ND = not detected.

DMD Fast Forward. Published on November 28, 2006 as DOI: 10.1124/dmd.106.011551
This article has not been copyedited and formatted. The final version may differ from this version.

TABLE 4

Rates of Formation of the Monohydroxylated Metabolites of MK-0524, **M1** and **M4**, by Recombinant Human CYPs [a]

CYP	M1 (pmol / pmol*hr)	M4 (pmol / pmol*hr)
1A1	0.09	0.2
2A6	nd[b]	Nd
2C9	1.9	2.4
2C19	nd	0.17
2D6	nd	Nd
2E1	nd	Nd
3A4	19.2	27

[a] MK-0524 (10 μM) was incubated for 90 min with CYP microsomes (20 pmol P450) in the presence of NADPH at 37°C. Values represent mean; n = 2

[b] nd = not detected

DMD Fast Forward. Published on November 28, 2006 as DOI: 10.1124/dmd.106.011551
This article has not been copyedited and formatted. The final version may differ from this version.

TABLE 5

LC-MS/MS Analysis of Metabolites of MK-0524

Metabolite	*m/z*	Fragment Ions, *m/z*
MK-0524	434	416, 390, 278
M1	450	432, 406, 388
M2	610	434, 416, 390, 278
M3	448	430, 404, 376
M4	450	432, 406, 388
M5	326	308, 282, 264
M7	432	388, 262
M9, M10, M11, M12	626	432, 406, 388

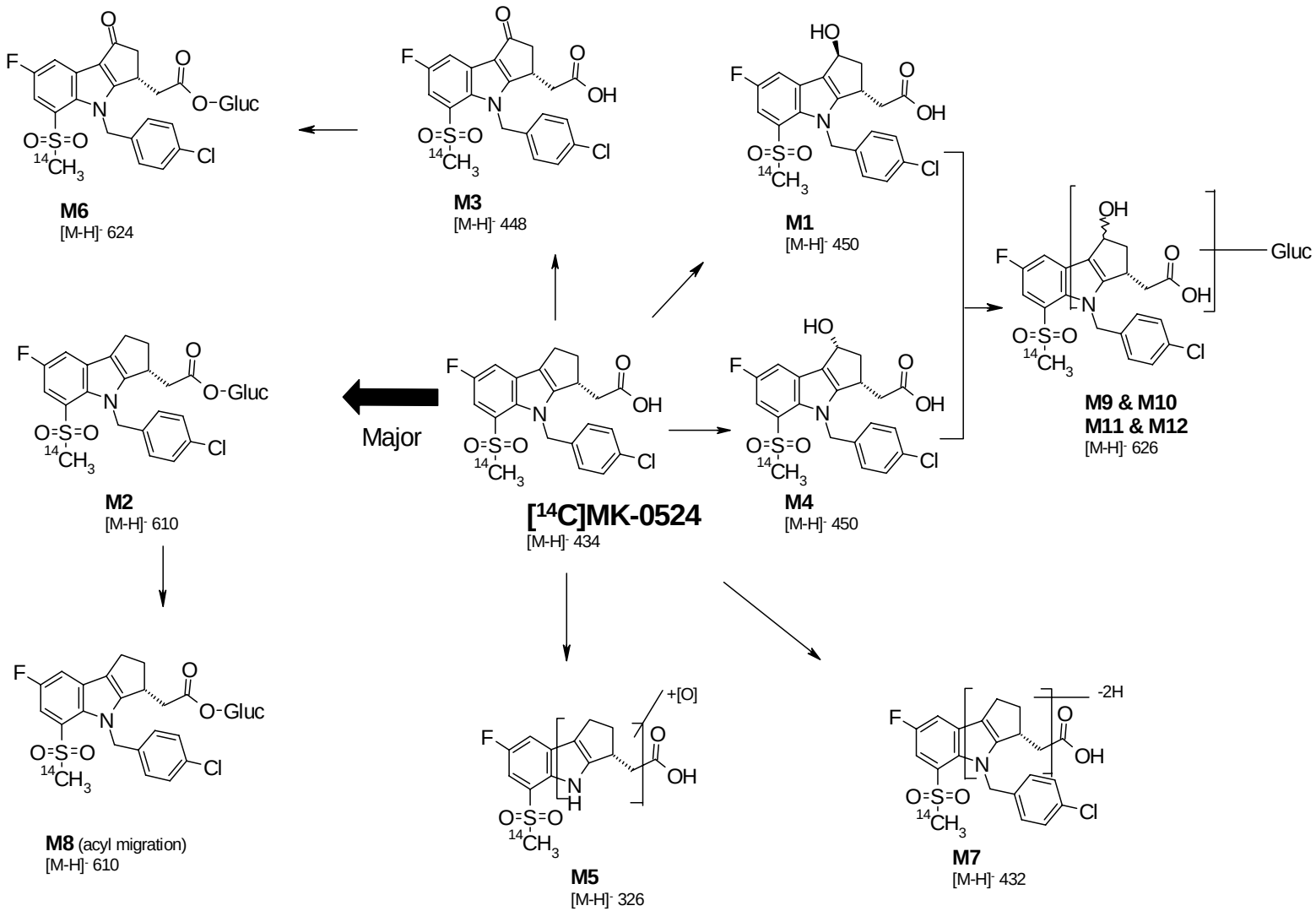

Fig 1

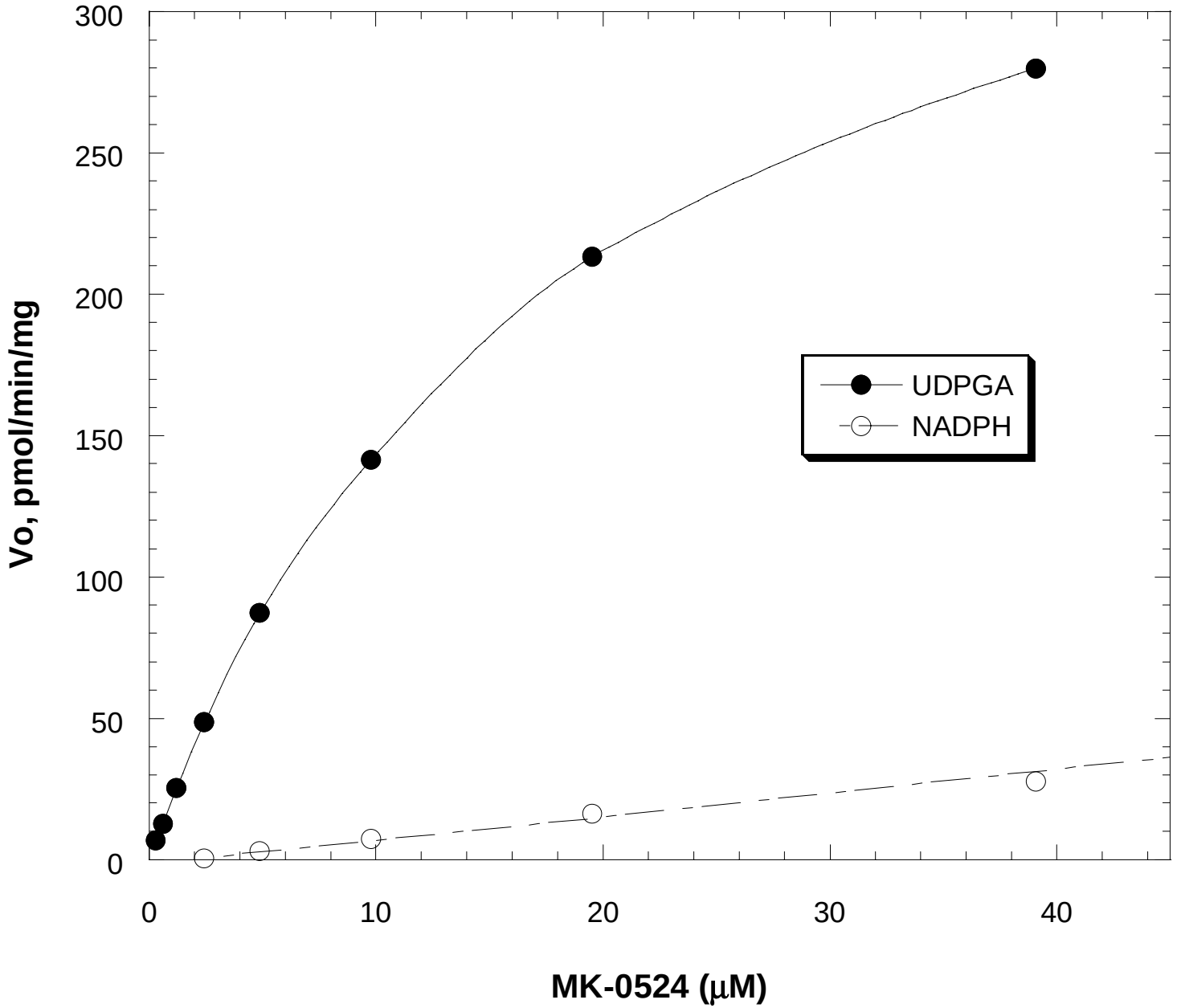

Fig. 2

DMD Fast Forward. Published on November 28, 2006 as DOI: 10.1124/dmd.106.011551
This article has not been copyedited and formatted. The final version may differ from this version.

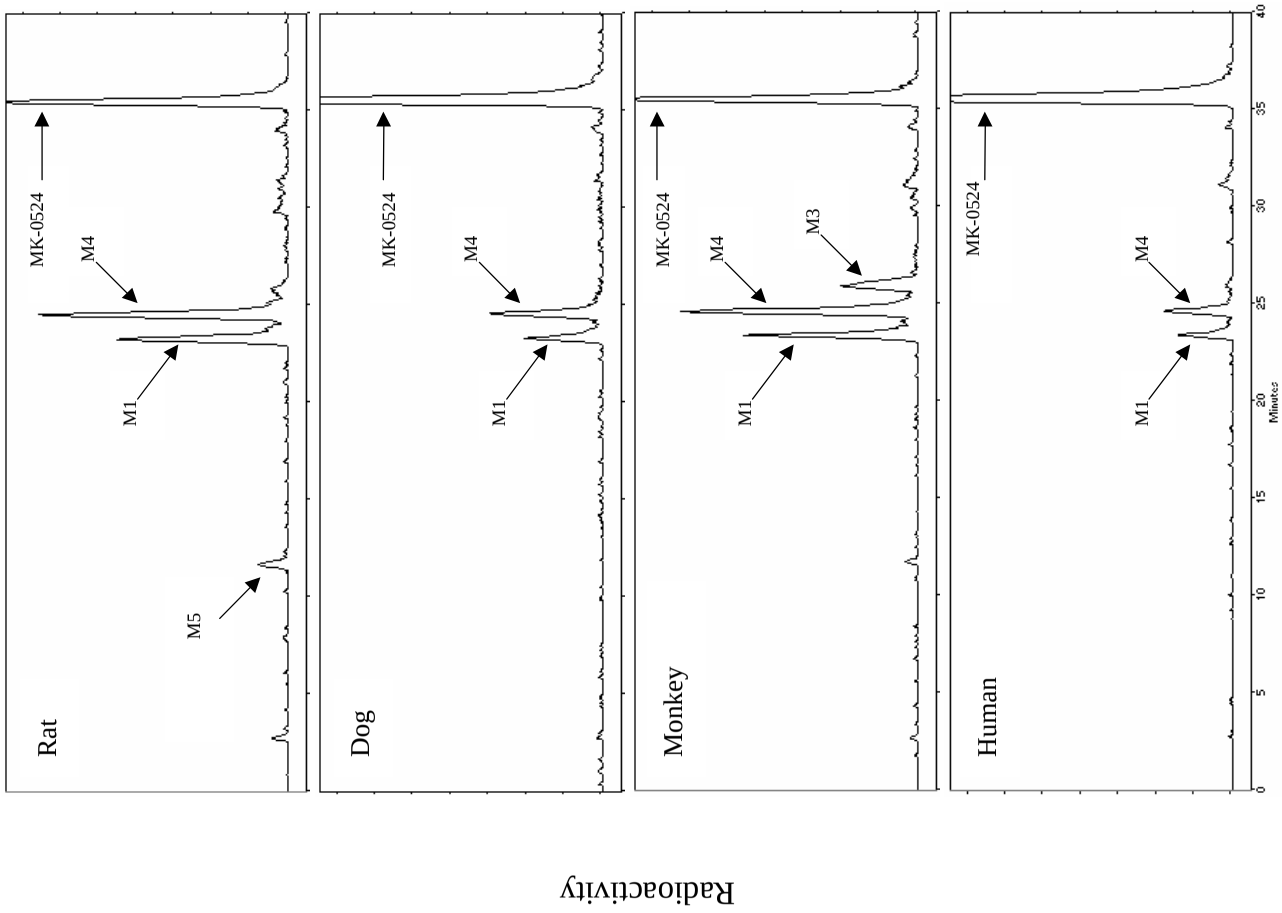

Fig. 3

DMD Fast Forward. Published on November 28, 2006 as DOI: 10.1124/dmd.106.011551
This article has not been copyedited and formatted. The final version may differ from this version.

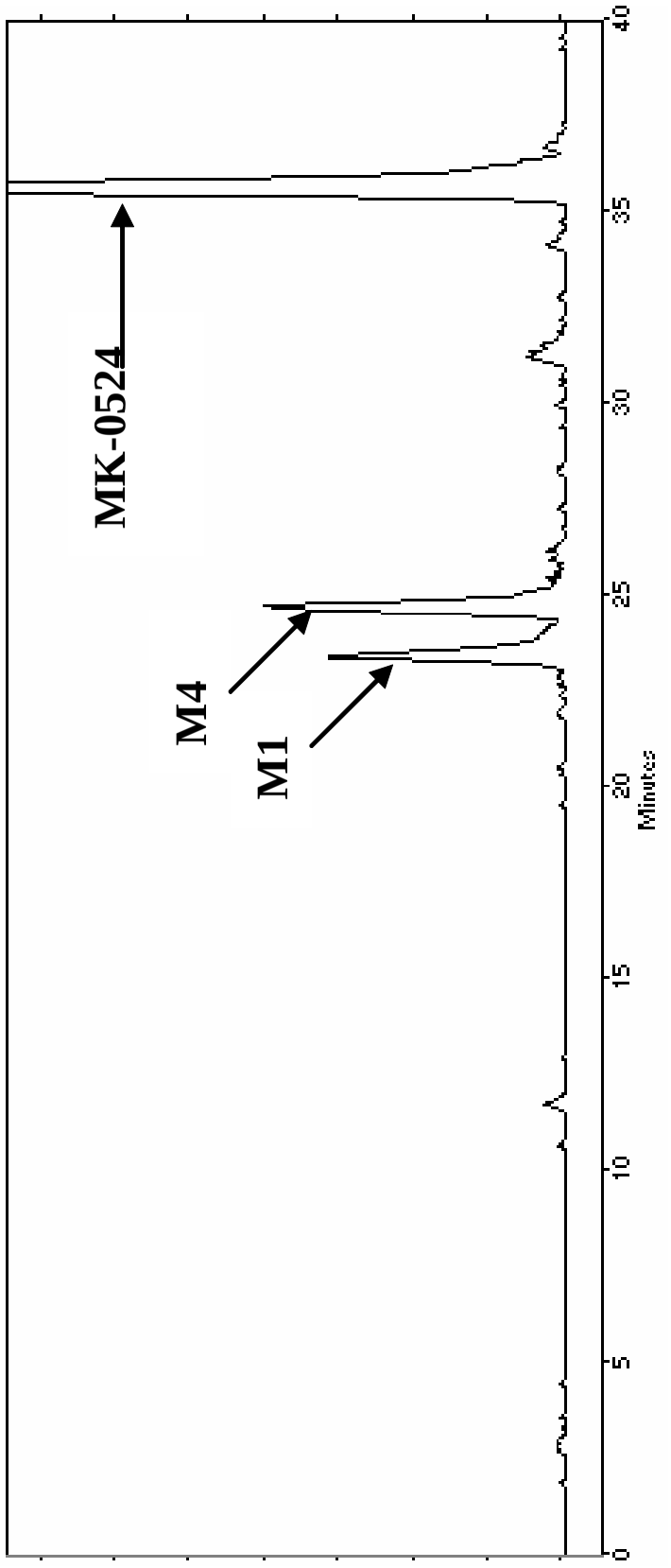

Fig 4

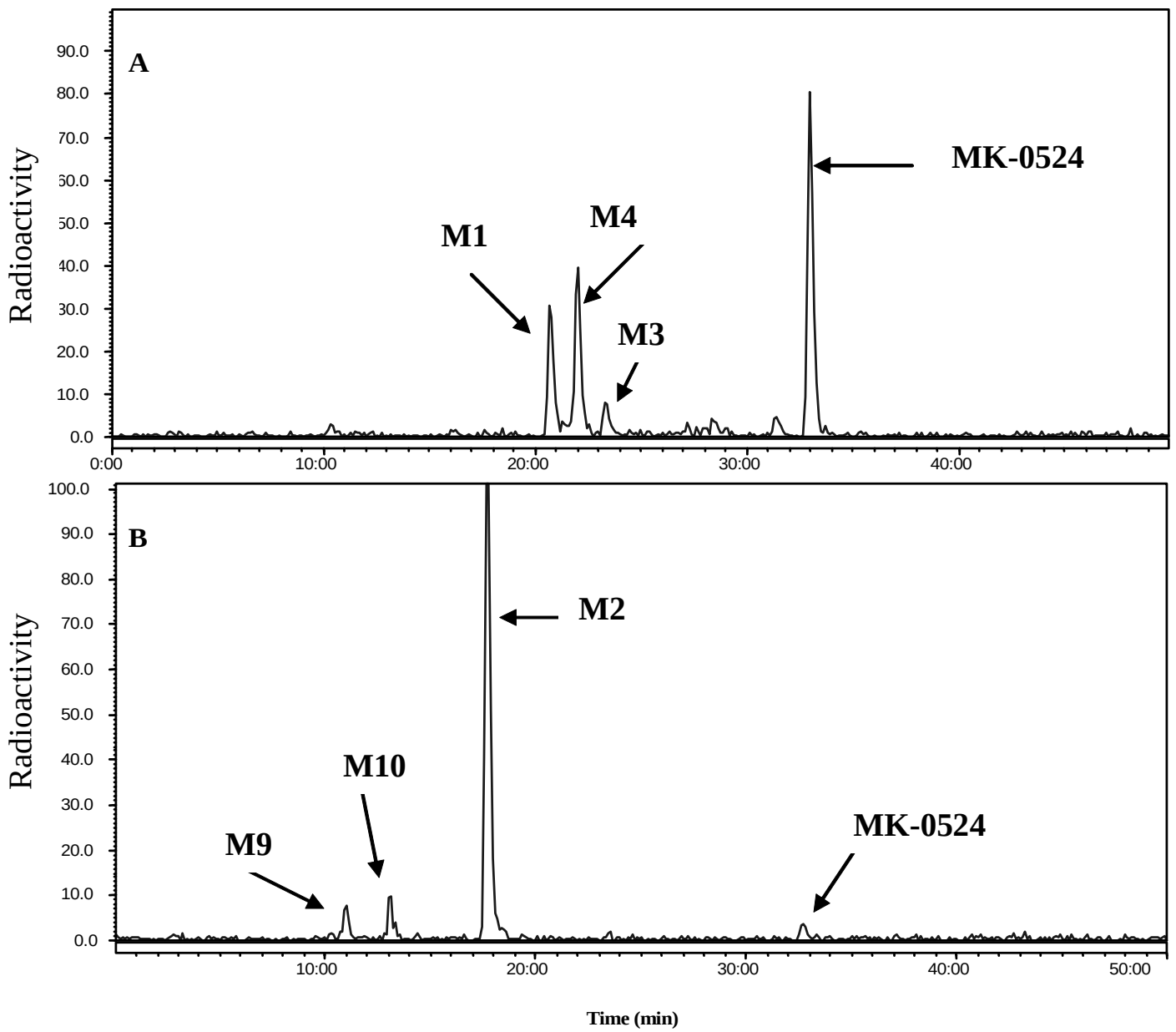

Fig 5

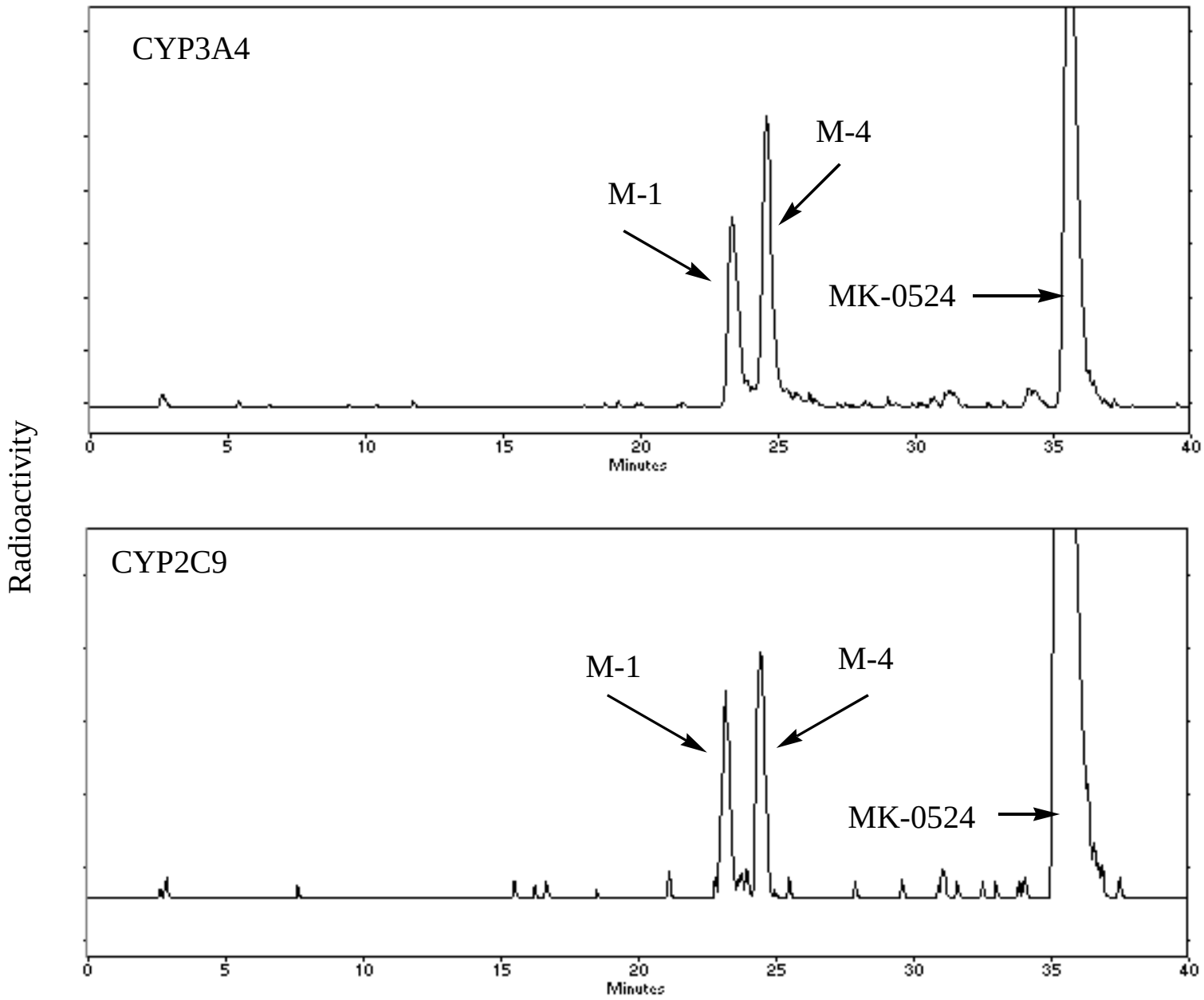

Fig 6

DMD Fast Forward. Published on November 28, 2006 as DOI: 10.1124/dmd.106.011551
This article has not been copyedited and formatted. The final version may differ from this version.

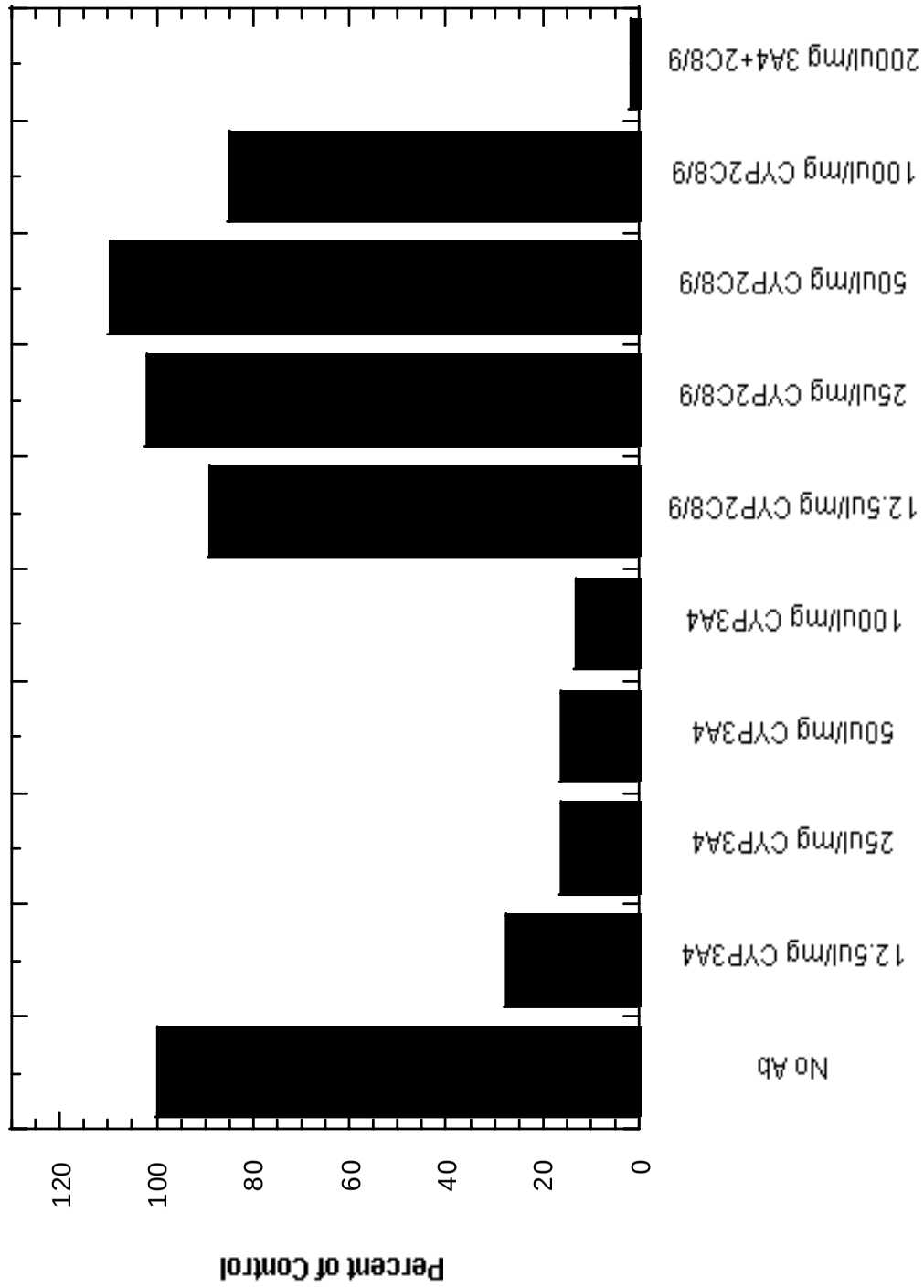

Fig 7

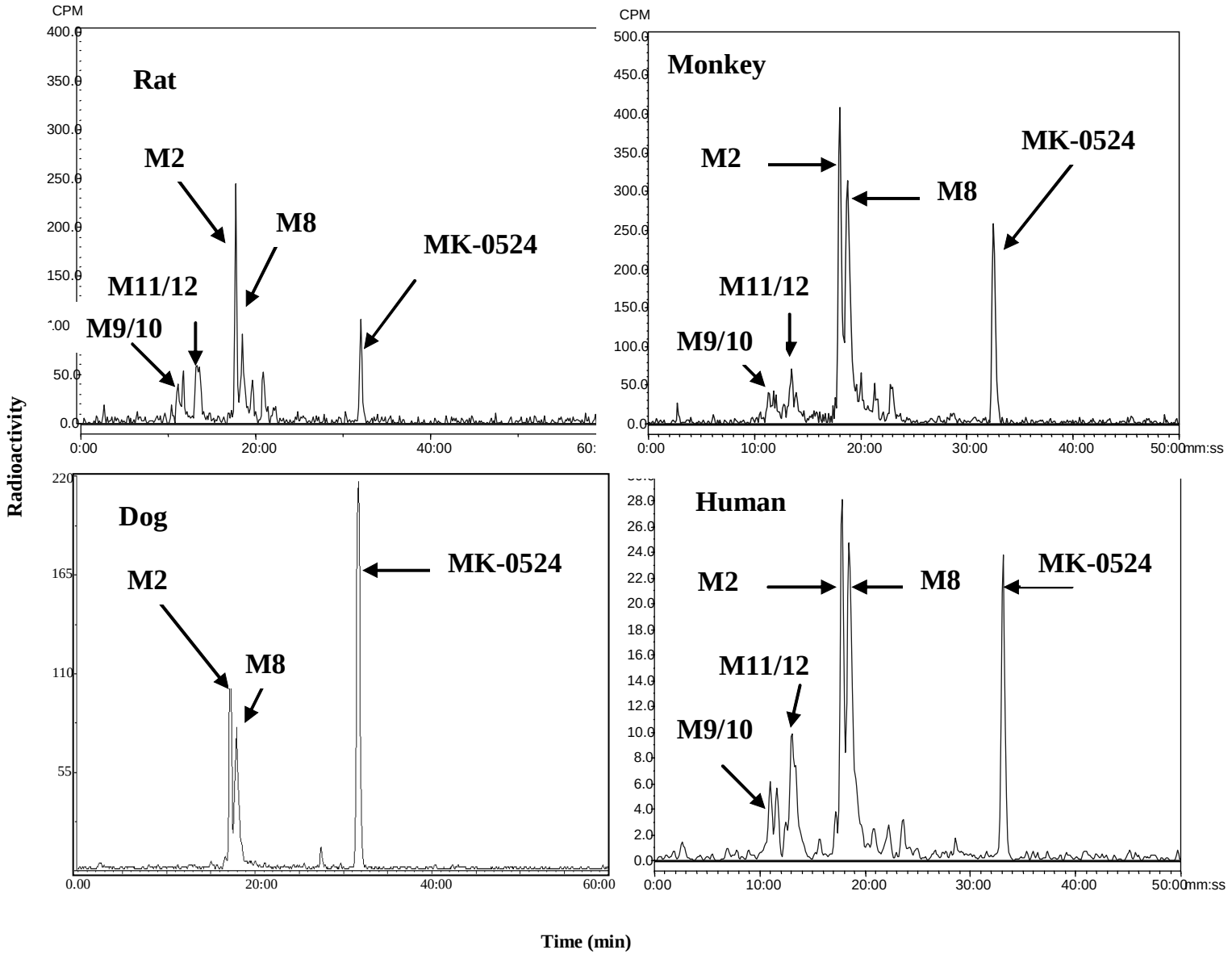

Fig 8

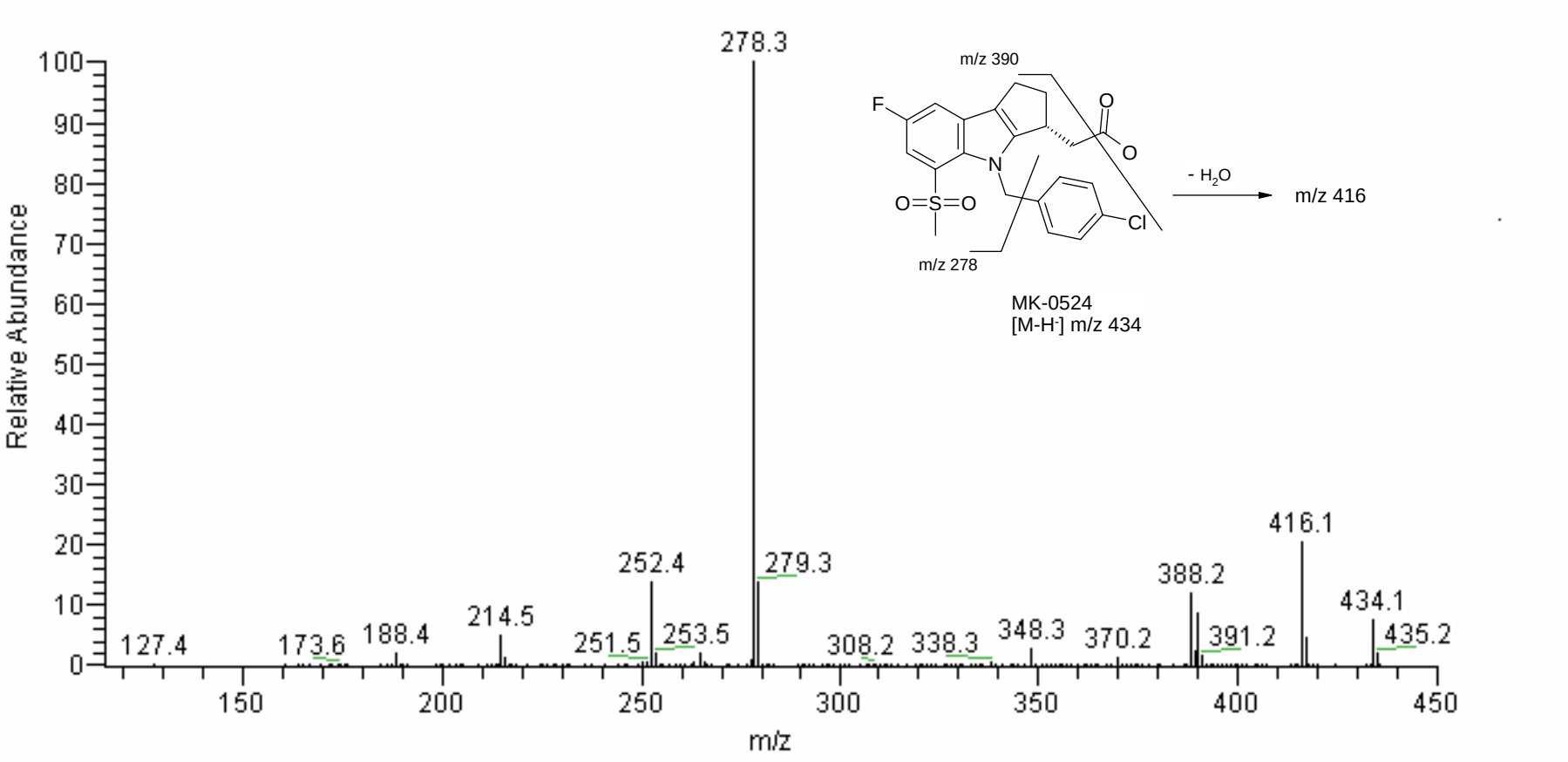

Fig 9